Direct imaging of both ferroelectric and antiferromagnetic domains in multiferroic $BiFeO_3$ single crystal using x-ray photoemission electron microscopy

R. Moubah,[1,a)] M. Elzo,[2,3] S. El Moussaoui,[4] D. Colson,[1] N. Jaouen,[2] R. Belkhou,[2] and M. Viret[1]
[1]*Service de Physique de l'Etat Condensé, URA CNRS 2464, CEA Saclay, 91191, Gif-sur-Yvette, France*
[2]*Synchrotron Soleil, Saint-Aubin, 91192, Gif-sur-Yvette BP 48, France*
[3]*Institut Néel, CNRS/UJF, 38042, Grenoble, France*
[4]*Paul Scherrer Institut, Swiss Light Source, Villigen, CH-5232, Switzerland*

(Received 24 October 2011; accepted 17 December 2011; published online 24 January 2012)

In this work, we propose to study the magnetic and ferroelectric configurations in ferroelectric multidomain $BiFeO_3$ single crystals. Using x-ray (magnetic) linear dichroism in a photoemission electron microscope (X-PEEM), we are able to directly image both the antiferromagnetic and ferroelectric domains. We find that inside one single ferroelectric domain several antiferromagnetic domains coexist. This is different from what was observed on epitaxial thin films, where the ferroelectric domains perfectly match the antiferromagnetic ones, but also from previous neutron measurements on ferroelectric monodomain single-crystals for which one single antiferromagnetic domain was identified. This underlines the fundamental differences between thin films, bulk samples, and single versus ferroelectric multidomain samples. © *2012 American Institute of Physics*. [doi:10.1063/1.3679101]

Magnetoelectric coupling enables to control the magnetization of a material by an electric field or its electric polarization by a magnetic field. Understanding such coupling in multiferroic materials is an important task at both fundamental and technological levels.[1–5] Up to now, $BiFeO_3$ is the most promising multiferroic exhibiting such phenomenon above room temperature,[1] making it an excellent candidate for potential applications as magnetic memory-storage cells.[2] This compound is non-centrosymmetric with a rhombohedral distortion with high temperature orders.[3] It is antiferromagnetic (AFM) with a periodic arrangement of the spins following a cycloid. The AFM and ferroelectric (FE) polarization vectors are linked, and the magnetic moments rotate in a plane containing the direction of polarization P_s and the cycloidal propagation vector.[4] This coupling between the two orders opens the way to the control of magnetism by an electric-field, a property of great interest.[1–5] However, in $BiFeO_3$ single crystals, the magnetoelectric coupling does not impose a unique cycloidal propagation vector in each polarization domain. Hence, it is important to study the interaction of the different orders at a local microscopic level. In this respect, x-ray photoelectron emission microscopy (X-PEEM) using x-ray synchrotron light is one of the most powerful and suitable techniques allowing to image several order parameters including ferroelectricity, ferromagnetism, and antiferromagnetism. So far, only "conventional" AFM domains in $BiFeO_3$ thin films were imaged using X-PEEM.[1] Thin films' results cannot be extrapolated to single crystals, because they do not exhibit the characteristic AFM cycloid, which is made unstable due to the strain imposed by the substrate. In order to carry out similar measurements in single crystals, one has to face several experimental difficulties such as their small size (a few hundreds of μm) and above all the large charge build-up effect that can hinder the X-PEEM measurements. In the present study, we report on the imaging of both AFM and FE domains in a $BiFeO_3$ single crystal in a multidomain state. Our finding is that inside one single FE domain several AFM domains can coexist. This result differs not only from what was observed on epitaxial thin films,[1] where the FE domains perfectly matches the AFM ones,[1] but also from previous neutron measurements on FE monodomain single crystals for which one single AFM domain was identified.[4] This underlines the fundamental differences between thin films, bulk samples, and single versus FE multidomain samples. Because X-PEEM imaging is essentially a surface measurement, our present results are also relevant for understanding the exchange coupling at the interface between $BiFeO_3$ single crystals and deposited ferromagnetic layers.[5]

Using a flux technique, we have synthesized high quality $BiFeO_3$ single crystals. As grown, most crystals are FE monodomains,[6] where the polarization lies along the long (111) diagonals of the pseudocubic unit cell. For this study, we choose a 0.8 mm long, 0.36 mm wide, and 0.05 mm thick FE multidomain $BiFeO_3$ single crystal. To avoid charging problems due to the highly insulating nature of our crystals, a gold layer was deposited on the sample in a pattern with holes in order to evacuate charges from most of the crystal's surface while still allowing the pure crystal to be probed. Furthermore, during the X-PEEM measurements, a high intensity UV lamp is used to enhance the conductivity of the sample. The low energy electron microscopy (LEEM)-PEEM set up at the SIM beamline of the Swiss Light Source[7] was used to obtain the images and the energy spectra in two operating modes XLD and XMLD. XMLD contrast images are created combining X-PEEM images obtained at two energy points of the Fe $L_{2A,B}$ multiplet using horizontally and vertically polarized x-ray, through the quantity $(I_1 - I_2)/(I_1 + I_2)$, where I_1

a)Electronic mail: Reda.Moubah@cea.fr.

and I_2 are the images obtained at the Fe L_{2A} and L_{2B} edges, respectively. The contrast obtained from XMLD-PEEM with vertical linear polarization (VLP) maps the in-plane component of the AFM domains while the contrast with horizontal linear polarization (HLP) represents the out-of-plane one. For the XLD-PEEM contrast, we used the difference between HLP and VLP of the incident x-ray vector at the O_{1s} edge. All measurements were carried out at a temperature of 325 K and a vacuum lower than $5 \cdot 10^{-9}$ mbar.

We primarily study the visible polarization domains in a single crystal using polarized light microscopy (PLM) as shown in Figure 1(a) where domains in the tens of microns size can be observed. The contrast between bright and dark areas comes from the birefringence of the FE domains. Because the light impinges on the sample at normal incidence, the contrast in the image only originates from the in-plane components of polarization directions (it is independent of the sign of the polarizations). No perpendicular information can be measured, and the inferred projected domain pattern is shown in the Figure 1(a). A crack can be seen at the crossing of the FE domains, as confirmed in the scanning electron micrograph (SEM) of Fig. 1(b). It is most likely caused by strain at the intersection of the different ferroelastic domains.

In order to get the complementary information necessary to identify the 3D polarization directions, we use X-PEEM to image the FE and AFM domains structure of $BiFeO_3$ using respectively X(M)LD (x-ray (magnetic) linear dichroism) effects at the O_{1s} and Fe $L_{2A,B}$. The 100% linearly polarized x-rays impinge on the sample at a grazing angle of 16°, and the x-ray polarization axis could be rotated continuously through a 90° range from purely VLP to HLP. In this configuration, the VLP lies within the sample surface plane while the HLP is perpendicular to it. The XLD allows to probe essentially the charge anisotropies, while the XMLD is sensitive to both the charge anisotropies and the AFM magnetic moment. From the XLD-PEEM images probed at the O_{1s} edge using the difference between HLP and VLP of the incident x-ray vector [Fig. 2(a)], the FE domain structures have been compared to the ones imaged in PLM in the same area as in Fig. 1(a). The strong resemblance of these two images indicates clearly that the observed features are due to the sample polarization. Because the x-ray beam impinges at 16° from the sample's surface (asymmetrical geometry), the projection of the light polarization on the sample allows for a contrast between domains with the same

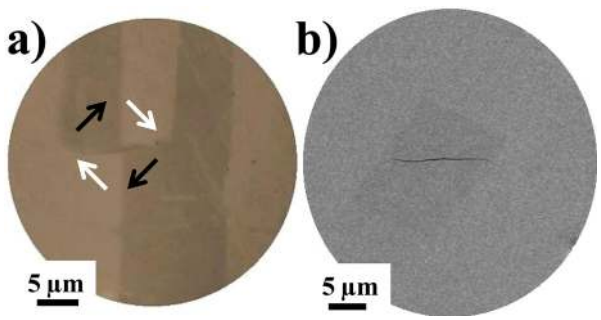

FIG. 1. (Color online) Optical PLM image of a FE multidomain $BiFeO_3$ single crystal (a). SEM image showing the crack at the intersection of the ferroelastic domains (b). The two micrographs were taken at the same region of the sample.

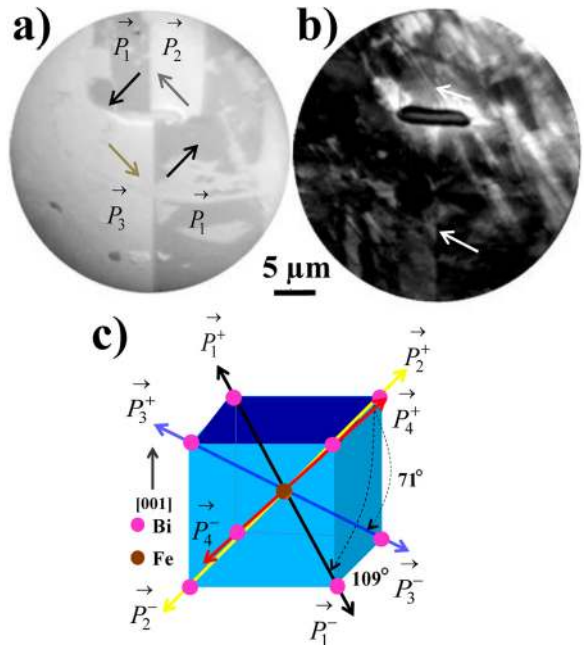

FIG. 2. (Color online) X-PEEM images taken on a $BiFeO_3$ single crystal. This figure allows to image: FE domains probed at the O_{1s} edge by subtracting the VLP and HLP images (a), AFM domains structure measured using the XMLD effect at the Fe $L_{2A,B}$ edge with HLP (b). The white arrows allow to distinguish the borders between the different FE domains. Illustration in the pseudocubic system of the crystal structure and the eight possible orientations of the FE polarization vectors variants, the blue plane shows the (001) plane parallel to the crystal surface (c).

in-plane polarization directions but a different out of plane component, using the HLP. A careful analysis of the image of Figure 2(a) allows to distinguish two different contrasts in the two white domains and a unique one in the black domains. We attribute this to a different out of plane component of the white domains and infer in three dimensions the polarizations in each domain, as presented in Figure 2(c). It should be noted that a large area in the bottom right domain of Figure 2(a) can be seen with a bright contrast not observed with PLM. This is likely due to charging artifacts, topological variations, or even adsorbates on the surface, which can significantly influence the photoelectron yield and then the contrast in X-PEEM. Indeed, the measured photoelectrons only come from a depth of a few nm, which leads to an extremely high surface sensitivity, while the visible microscope probes a larger depth (few tens μm). However, the similarity of the PLM and X-PEEM images provides a reliable indication that the in-plane FE domains structure is identical at the surface and in the bulk. Recently, Martí *et al.*[8] have evidenced the existence of a 10 nm thick skin layer of different electron density at the surface of $BiFeO_3$ single crystals.[8] Our measurements demonstrate that the potential presence of this layer does not modify the FE domain structure in $BiFeO_3$. We note that the FE domain structures have never been imaged in $BiFeO_3$ using the X-PEEM technique.[1] Considering the AFM contrast achievable using XMLD-PEEM at the Fe edge, this opens the way of correlating the FE domains to the AFM ones measured on the same area. In multiferroic materials, both antiferromagnetism and ferroelectricity participate to the contrast at the Fe edge when using the linear polarization. The proportion of each

term is hard to estimate, and it depends on the orientations of their respective vectors, their magnetic moment, and exchange/crystal field. Figure 2(b) is an image containing AFM contrast obtained by subtracting two images measured at two features of the Fe $L_{2A,B}$ edge with HLP. The magnetic signal being much smaller than the "ferroelectric" one, the obtained image is of worse quality than those taken at the O_{1s} edge in pure XLD [Figure 2(a)]. Any surface irregularity, contaminant, charge pockets, or weak XMLD effect generates a contrast which masks the interesting signal. It is therefore hard to visualize the real topology of AFM domains in $BiFeO_3$. By comparing the image of the FE domain structures [Fig. 2(a)], some correlations are visible as the borders between the different FE domains can be seen (indicated by arrows in Figure 2(b)). In order to check the magnetic nature of the different shapes seen on the figure, the angular dependence of the XMLD effect is essential as the magnetic contrast depends on the mutual orientation of the x-ray polarization and the AFM vectors. In general, a dark color indicates that the AFM vector is parallel to the x-ray polarization vector, and white perpendicular, with a grey contrast in-between. In our case, the situation is slightly more complicated because in $BiFeO_3$ the AFM vectors form cycloidal patterns, as shown in Figure 3(a). Therefore, one can define "dense" AFM planes in which the AFM vectors rotate and the associated perpendicular directions with an "absent" AFM contribution. When the cycloid planes intersect the top (001) surface of the crystal, they make dense and absent directions perpendicular to each other which induce a bright/dark contrast in XMLD. The images recorded at different in-plane angles between the vertical polarization and a (001) crystal direction are shown in Figure 4. The gradual rotation of this angle from 0 to 45° induces a progressive change of the images contrast in certain areas, but in other regions, the contrast does not change, indicating that the information is masked. We attribute this to the weakness of the XMLD effect and the presence, at the surface, of either adsorbates or inhomogeneously charged areas, which mask the underlying AFM domains. However, we can conclude that several AFM domains exist in a single FE domain. The angular contrast variation of some regions is opposite [areas surrounded by red and blue colors in Figs. 4(a) to 4(d), these images were taken from the dashed circle defined in Figure 4(e)], thus indicating clearly that their AFM vectors are differently oriented within a unique FE domain.

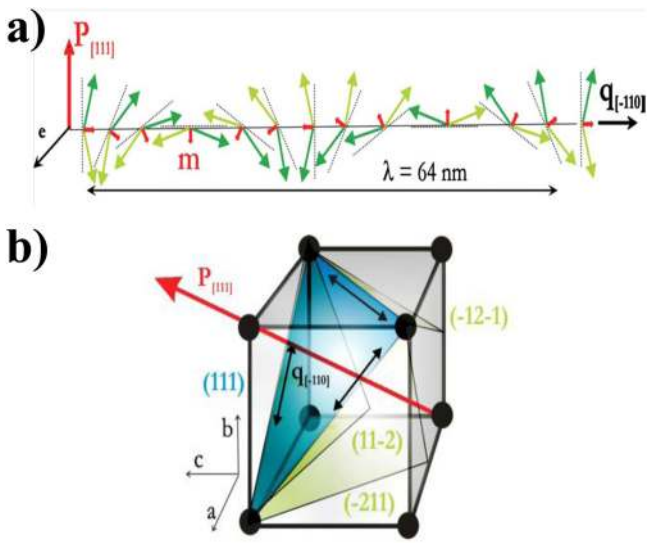

FIG. 3. (Color online) Schematics of the 64 nm AFM cycloid (a), as reported in Ref. 12. The moments lie in the plane defined by the AFM spiral vectors and the polarization direction. Schematics in the pseudocubic structure of the (111) plane containing the three possible [101] cycloid propagation vectors in a single FE domain (b), and their relationship with the FE polarization vector (P). The magnetic moments are contained in one of the (121) planes.

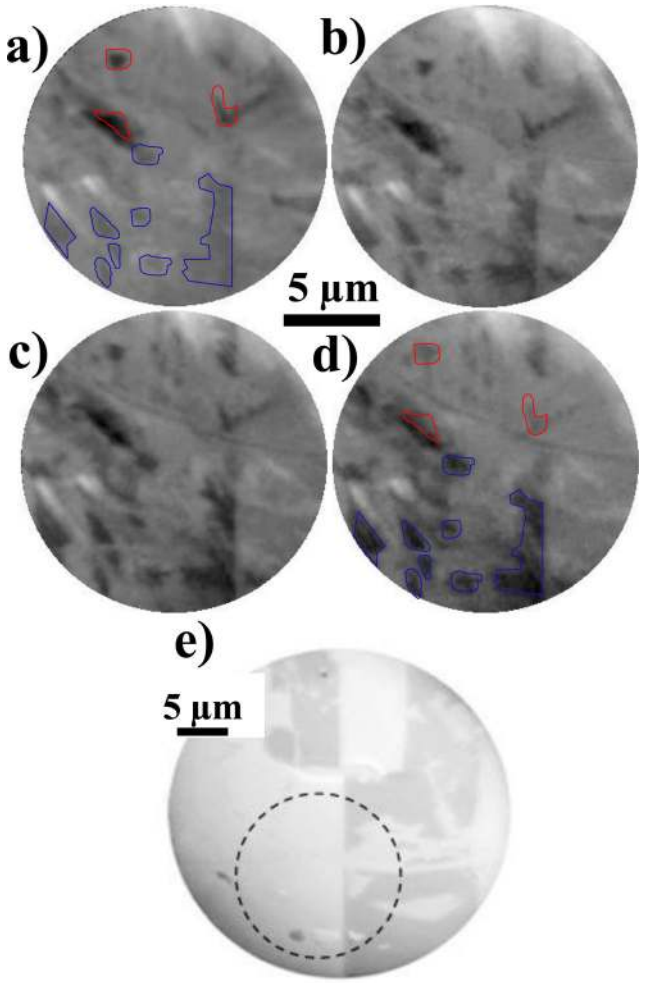

FIG. 4. (Color online) X-PEEM images in the XMLD mode obtained at the Fe $L_{2A,B}$ edges with VLP, on a $BiFeO_3$ single crystal by rotating the in plane angle by: 0° (a), 15° (b), 30° (c), 45° (d). Regions surrounded by red and blue, highlight AFM domains with opposite angular contrast variation inside a single FE monodomain. These images were taken from the dashed circle defined in (e) (between two FE monodomains).

In order to support these results, we recorded several absorption spectra at the Fe edge with HLP, from areas surrounded by red and blue colors of Figure 4. Figures 5(a) and 5(b) present spectra obtained at different angles, 0 to 45°, respectively. In both cases, two distinct peaks situated at around 722.8 and 724.2 eV are observed, which correspond to the degenerated multiplets structure of the Fe $L_{2A,B}$ edge. The comparison between the spectral shapes of the XAS shows a weak but obvious angular variation, which can be partly attributed to the expected $\cos^2$ dependence with the angle between the AFM cycloidal planes and the x-ray linear polarization. The weakness of the XMLD effect (also due to

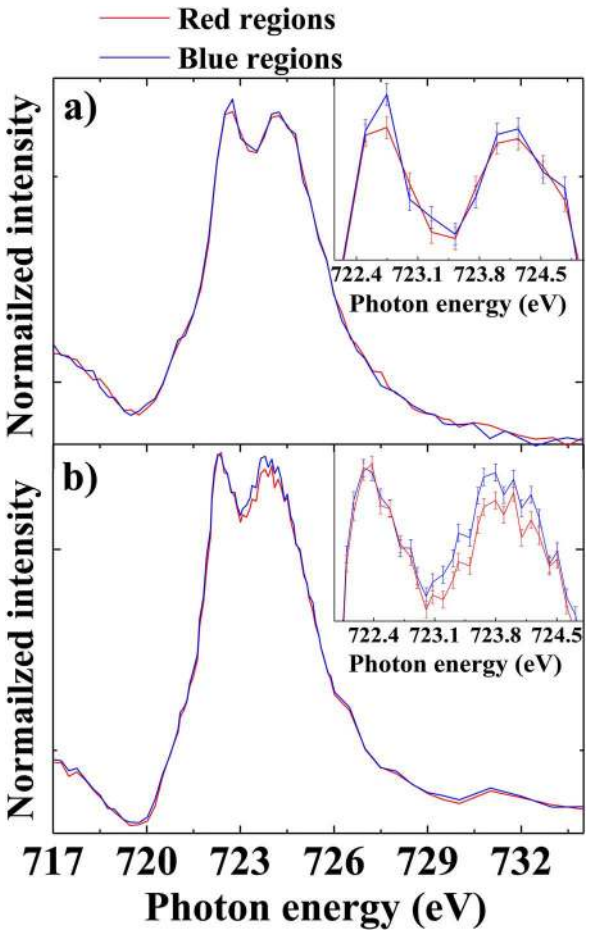

FIG. 5. (Color online) X-ray absorption spectra at the Fe $L_{2A,B}$ edge, recorded from areas surrounded by red and blue in Figures 4(a) and 4(b), present the spectra obtained by rotating the in plane angle by 0° (a) and 45° (b), respectively. The incident x-ray polarization vector is vertical. The insets show zooms of the curves around the two main peaks, evidencing the small but measurable difference in their intensities.

the fact that the AFM vectors form cycloidal patterns) is responsible for the problems to image the real topology of the AFM domains. It is important to point out that in conventional AFM oxides such as NiO or Fe_2O_3, the XMLD contrast is mainly imposed by charge anisotropy. The alignment of the local atomic spins along this axis breaks the charge symmetry by spin orbit coupling, inducing a small anisotropy, which leads to an asymmetry of the x-ray absorption signal. Thus, in these systems, probing the charge anisotropy allows to measure the AFM axis. The rotation of AFM moments in BFO dilutes the magnetic signal and makes the XMLD measurements difficult, also in contrast to what happens in thin films[9] where AFM domains can be more easily imaged.[1]

Our magnetic measurements are qualitatively different from those in thin films, for which it was found that each FE domain corresponds only to one AFM domain.[1] This underlines the general difference in properties between thin films, and multidomain single crystals: (i) In bulk samples, because of the rhombohedral symmetry, there exist three equivalent variants of the propagation vectors for the cycloidal rotation: $q_1(\delta,0,-\delta)$, $q_2(0,\delta,-\delta)$, and $q_3(-\delta,\delta,0)$, where $\delta = 0.045$, as shown in Figure 3(b). In thin films, this cycloid is destroyed, and the AFM vector has no variants.[9] (ii) As grown, the $BiFeO_3$ thin films were shown to be in a FE multidomain state, with a small domain size below 100 nm,[10] which is likely to preclude the presence of even smaller AFM domains. We recall here that as grown, most our $BiFeO_3$ single crystals are FE and AFM monodomains,[4,6] and only a few of them (less than 10%) become FE multidomains due to the application of random pressure during mechanical extraction via the strong magnetoelastic effect in $BiFeO_3$.

Three of our monodomain single crystals have been measured by neutron scattering and found to be also mostly AFM monodomains.[4] Some other measurements such as Raman scattering are also consistent with the single AFM domain state for as-grown crystals.[11] Here, our present sample is in a FE multidomain state. As ferroelectric switching drives to reorientation of the AFM order,[1] the transformation from the monodomain to multidomain FE states is likely to be responsible for the creation of different AFM structures. Because for each ferroelectric domain, there exist three equivalent propagation vectors for the cycloidal rotation (and three planes in which the AFM vector rotates), the switching from the FE monodomain to multidomain states could lead to the creation of several variants of AFM domains inside each FE domain.

In summary, we have investigated the magnetic and FE configurations in a FE multidomain $BiFeO_3$ single crystal using X-PEEM in XLD and XMLD modes. Resolved imaging reveals the existence of several AFM domains inside each larger FE domain. This is consistent with the existence of the three energetically equivalent variants of the cycloidal directions of rotating AFM vectors within a single polarization domain. These results should be of great interest to improve the comprehension of the magnetoelectric coupling in the $BiFeO_3$ bulk samples.

This research project has been supported by the European Commission under the 7th Framework Programme: Research Infrastructures. Grant Agreement Number 226716. We also acknowledge the support from the French RTRA contract "MULTIFERRO." We thank SIM beamline staffs at PSI for their support.

[1]T. Zhao, A. Scholl, F. Zavaliche, K. Lee, M. Barry, A. Doran, M. P. Cruz, Y. H. Chu, C. Ederer, N. A. Spaldin, R. R. Das, D. M. Kim, S. H. Baek, C. B. Eom, and R. Ramesh, Nature Mater. **5**, 823 (2006).
[2]G. Catalan and J. F. Scott, Adv. Mater. **21**, 2463 (2009).
[3]G. Smolenskii and I. Chupis, Sov. Phys. Usp. **25**, 475 (1982).
[4]D. Lebeugle, D. Colson, A. Forget, M. Viret, A. M. Bataille, and A. Gukasov, Phys. Rev. Lett. **100**, 227602 (2008).
[5]D. Lebeugle, A. Mougin, M. Viret, D. Colson, and L. Ranno, Phys. Rev. Lett. **103**, 257601 (2009).
[6]D. Lebeugle, D. Colson, A. Forget, and M. Viret, Appl. Phys. Lett. **91**, 022907 (2007).
[7]C. Quitmann, U. Flechsig, L. Patthey, T. Schmidt, G. Ingold, M. Howells, M. Janousch, and R. Abela, Surf. Sci. **480**, 173 2001.
[8]X. Martí, P. Ferrer, J. Herrero-Albillos, J. Narvaez, V. Holy, N. Barrett, M. Alexe, and G. Catalan, Phys. Rev. Lett. **106**, 236101 (2011).
[9]F. Bai, J. Wang, M. Wuttig, J. Li, N. Wang, A. P. Pyatakov, A. K. Zvezdin, L. E. Cross, and D. Viehland, Appl. Phys. Lett. **86**, 032511 (2005).
[10]J. Wang, J. B. Neaton, H. Zheng, V. Nagarajan, S. B. Ogale, B. Liu, D. Viehland, V. Vaithyanathan, D. G. Schlom, U. V. Waghmare, N. A. Spaldin, K. M. Rabe, M. Wuttig, and R. Ramesh, Science **299**, 1719 (2003).
[11]P. Rovillain, R. de Sousa, Y. Gallais, A. Sacuto, M. A. Méasson, D. Colson, A. Forget, M. Bibes, A. Barthélémy, and M. Cazayous, Nature Mater. **9**, 975 (2010).
[12]D. Lebeugle, A. Mougin, M. Viret, D. Colson, J. Allibe, H. Béa, E. Jacquet, C. Deranlot, M. Bibes, and A. Barthélémy, Phys. Rev. B **81**, 134411 (2010).